



Comparison of One-Focus and Two-Foci Setup in Single-Molecule Detection Experiments

JÖRG ENDERLEIN* and
RICHARD A. KELLER

*Chemical Science and Technology Division, MS M888,
Los Alamos National Laboratory, Los Alamos, New
Mexico 87545*

Index Headings: **Single-molecule detection; Flow cytometry; Laser-induced fluorescence**

INTRODUCTION

In recent years, single-molecule detection (SMD) in fluid flow has become a widely used technique in ultrasensitive fluorescence detection, (see, e.g., Ref. 1 and references therein). Some of the most promising applications are high-speed DNA sequencing,²⁻⁵ sizing of DNA fragments,⁶⁻⁸ genetic screening,^{9,10} diagnostics,^{11,12} and ultrasensitive chemical analysis.^{13,14}

The detection of a single molecule in a fluid flow at room temperature is a challenging task, which is due to several effects: the surrounding liquid and possible contamination in it cause high background signals; photobleaching effects restrict the overall number of detectable photons from one molecule; and diffusion can cause the molecule to miss the exciting laser beam when flowing along the capillary. With respect to many applications, such as rapid DNA sequencing, it is desirable to have a detection efficiency as high as possible for the molecules flowing through the capillary, which restricts the minimization of the excitation-detection volume, thus imposing limits for the decrease of the background signal.

There are different approaches for increasing the signal-to-background ratio in SMD experiments, among which are hydrodynamic focusing to reduce the sample stream diameter,¹⁵ application of time-resolved fluorescence techniques,^{16,17} and use of high-efficiency optical

filters for separating the scattered light from the fluorescence.¹⁸

One suggestion, which often occurs in the search for methods for enhancing the SMD efficiency, is the use of multiple excitation-detection regions along the capillary and the application of an analysis for correlating the photon detection data from the different regions. The basis of this approach is the recognition that a flowing molecule will cause a highly correlated fluorescence signal from consecutive excitation-detection regions, with a correlation time, on average, equal to the mean travel time of the molecule from one excitation-detection region to the next. In this note we demonstrate that, at a constant laser power, no improvement results from using time-correlated detection from multiple-foci regions. Although we will restrict ourselves to the analysis of single-molecule detection in this paper, the methods used and the obtained results will be valid for general flow detection experiments, including flow cytometry.

DISCUSSION

To demonstrate the general method of analysis, we first study a simple example. Two cases are considered:

1. Signal is collected from one detection region irradiated by an excitation laser at power P .
2. Signal is collected from two detection regions, each irradiated by an excitation laser at power $P/2$.

In the first case, photons are detected in one channel with Poissonian statistics with mean number m , and in the second case, photons are detected in two channels with Poissonian statistics with mean $m/2$ per channel. The schematic setup of the two-channel experiment is shown in Fig. 1. It is assumed that there is a uniform movement of the molecule along the flow axis, and no diffusion takes place. The signal in the second channel is collected at a time interval after the signal in the first channel, with the time interval equal to the travel time of the molecule between the two channels.

In both setups one has the two possible cases: pure background ($m = m_{bg}$) and background plus a molecule's fluorescence ($m = m_{bg} + m_{mol}$). The corresponding Poissonian probability distributions for each experiment are then

$$P_m(N) = \frac{m^N}{N!} \exp(-m) \quad (1)$$

Received 11 July 1996; accepted 25 September 1996.
*Author to whom correspondence should be sent.

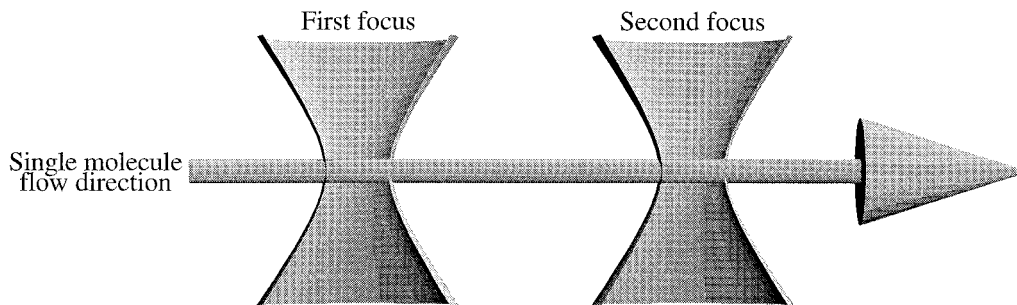


FIG. 1. Principal sketch of a two-foci experimental setup.

and

$$P_m(N_1, N_2) = \frac{(m/2)^{N_1+N_2}}{N_1!N_2!} \exp(-m) \quad (2)$$

with either $m = m_{bg}$ or $m = m_{bg} + m_{mol}$, and N, N_1, N_2 denoting the number of detected photons. To make a comparison between the two methods of detection, one has to calculate the accuracy with which one can distinguish a molecule from the background. The optimal method for doing this is by means of the maximum likelihood function (MLF).^{19–21} For a given experimental number of detected photons, the MLF is the logarithm of the ratio of the probability that this number was produced by a molecule plus background to the probability that the same number was produced by the background alone. Thus, for our example, the MLFs are

$$L_1 = N \log \left(1 + \frac{m_{mol}}{m_{bg}} \right) - m_{mol} \quad (3)$$

in the one-channel experiment and

$$L_2 = (N_1 + N_2) \log \left(1 + \frac{m_{mol}}{m_{bg}} \right) - m_{mol} \quad (4)$$

in the two-channel experiment.

To perform an error analysis of both experimental setups, one has to calculate the probability distributions for L_1 and L_2 for the cases of pure background and of pure background plus molecule. These are given by

$$\begin{aligned} P_m(L_1) &= \sum_{N=0}^{\infty} P_m(N) \delta \left(L_1 - N \log \left(1 + \frac{m_{mol}}{m_{bg}} \right) + m_{mol} \right) \\ &= \int_{-\infty}^{\infty} \frac{dk}{2\pi} \sum_{N=0}^{\infty} \frac{m^N}{N!} \exp \left[ikL_1 - ikN \log \left(1 + \frac{m_{mol}}{m_{bg}} \right) \right. \\ &\quad \left. - ikm_{mol} - m \right] \\ &= \int_{-\infty}^{\infty} \frac{dk}{2\pi} \exp [ik(L_1 - m_{mol}) - m + m \\ &\quad \cdot \exp(-ik \log(1 + m_{mol}/m_{bg}))] \end{aligned} \quad (5)$$

in the one-channel setup and by

$$\begin{aligned} P_m(L_2) &= \sum_{N_1=0}^{\infty} P_{m/2}(N_1) \sum_{N_2=0}^{\infty} P_{m/2}(N_2) \\ &\quad \cdot \delta \left(L_2 - (N_1 + N_2) \log \left(1 + \frac{m_{mol}}{m_{bg}} \right) + m_{mol} \right) \\ &= \int_{-\infty}^{\infty} \frac{dk}{2\pi} \sum_{N_1=0}^{\infty} \frac{(m/2)^{N_1}}{N_1!} \sum_{N_2=0}^{\infty} \frac{(m/2)^{N_2}}{N_2!} \\ &\quad \cdot \exp \left[ikL_2 - ik(N_1 + N_2) \log \left(1 + \frac{m_{mol}}{m_{bg}} \right) \right. \\ &\quad \left. - ikm_{mol} - m \right] \\ &= \int_{-\infty}^{\infty} \frac{dk}{2\pi} \exp [ik(L_2 - m_{mol}) - m \\ &\quad + m \exp(-ik \log(1 + m_{mol}/m_{bg}))] \end{aligned} \quad (6)$$

in the two-channel setup. In both cases, the subscript m can have the value m_{bg} and $m_{bg} + m_{mol}$, according to the two cases of pure background and background with molecule, respectively. As can be seen from the last rows in Eqs. 5 and 6, the probability distributions of the MLF are identical for both experimental setups, which indicates that *both setups yield the same error rates for detecting the molecule*. There is nothing to be gained by using the two-foci setup and correlating the signal between the two regions.

In reality, however, two major complications arise in single-molecule detection experiments: the photodestruction of the fluorescing molecule during the detection process, and the diffusion of the molecule, causing escape from the detection volume. In the following, we concentrate on the role of photobleaching and neglect diffusion processes. We will make some comments about the role of diffusion at the end of this note.

The photodestruction of a single molecule complicates the exact description of the photon detection process significantly. In the absence of a single molecule, the photon detection probability is the same as above, namely, Eqs. 1 and 2, with $m = m_{bg}$. But the probability distributions in the case where a molecule is present now read (for details see Ref. 21):

$$\begin{aligned}
P_{\text{mol}}^{(1)}(N) &= \frac{1}{N!} \int_0^t dt_{\text{bl}} \dot{v}_{\text{bl}}(t_{\text{bl}}) v_{\text{f}}^N(t_{\text{bl}}) \\
&\quad \cdot \exp[-v_{\text{f}}(t_{\text{bl}}) - v_{\text{bl}}(t_{\text{bl}})] \\
&\quad + \frac{1}{N!} v_{\text{f}}^N(t) \exp[-v_{\text{f}}(t) - v_{\text{bl}}(t)] \quad (7)
\end{aligned}$$

for the one-channel setup, and

$$\begin{aligned}
P_{\text{mol}}^{(2)}(N_1, N_2) &= \delta(N_2) \int_0^t dt_{\text{bl}} \frac{\dot{v}_{\text{bl}}(t_{\text{bl}})}{2N_1!} \left(\frac{v_{\text{f}}(t_{\text{bl}})}{2} \right)^{N_1} \\
&\quad \cdot \exp \left[-\frac{v_{\text{f}}(t_{\text{bl}}) - v_{\text{bl}}(t_{\text{bl}})}{2} \right] \\
&\quad + \frac{1}{N_1!} \left(\frac{v_{\text{f}}(t)}{2} \right)^{N_1} \exp \left[-\frac{v_{\text{f}}(t) - v_{\text{bl}}(t)}{2} \right] \\
&\quad \cdot \int_0^t dt_{\text{bl}} \frac{\dot{v}_{\text{bl}}(t_{\text{bl}})}{2N_2!} \left(\frac{v_{\text{f}}(t_{\text{bl}})}{2} \right)^{N_2} \\
&\quad \cdot \exp \left[-\frac{v_{\text{f}}(t_{\text{bl}}) - v_{\text{bl}}(t_{\text{bl}})}{2} \right] \\
&\quad + \frac{1}{N_1!} \left(\frac{v_{\text{f}}(t)}{2} \right)^{N_1} \cdot \exp \left[-\frac{v_{\text{f}}(t) - v_{\text{bl}}(t)}{2} \right] \\
&\quad + \frac{1}{N_1! N_2!} \left(\frac{v_{\text{f}}(t)}{2} \right)^{N_1} \left(\frac{v_{\text{f}}(t)}{2} \right)^{N_2} \\
&\quad \cdot \exp[-v_{\text{f}}(t) - v_{\text{bl}}(t)] \quad (8)
\end{aligned}$$

for the two-channel setup, where the abbreviations

$$\begin{aligned}
v_{\text{f}}(t_{\text{bl}}) &= m_{\text{bg}} + \int_0^{t_{\text{bl}}} d\tau \mu_{\text{f}}(\tau) \\
v_{\text{bl}}(t_{\text{bl}}) &= \int_0^{t_{\text{bl}}} d\tau \mu_{\text{bl}}(\tau) \quad (9)
\end{aligned}$$

were used, with $\mu_{\text{f}}(\tau)$ and $\mu_{\text{bl}}(\tau)$ denoting the time-dependent fluorescence detection and photobleaching rates, respectively, and m_{bg} the mean number of detected background photons during the mean passage time t (through one focus). From Eqs. 9 it can be seen that $v_{\text{f}}(t_{\text{bl}})$ is the mean number of detected photons if the molecule is bleached at time t_{bl} , and $\exp[-v_{\text{bl}}(t_{\text{bl}})]$ is the probability that the molecule is not photobleached until time t_{bl} . In deriving Eqs. 7 and 8, it was again assumed that the signal from the second channel is collected with a time delay to the signal from the first channel with a delay equal to the travel time of the molecule from focus one to focus two. In Eq. 8, it was assumed that no photobleaching takes place between the two detection regions. For the sake of simplicity, we will assume that the detection efficiency is coordinate-independent over the complete volume of the focused laser beam. Then it occurs that $v_{\text{f}} - m_{\text{bg}} = \lambda v_{\text{bl}}$, with λ being the ratio of the product of overall detection efficiency and fluorescence

quantum yield to photobleaching quantum yield. With the use of the abbreviations

$$\begin{aligned}
x_t &= v_{\text{bl}}(t) \\
b &= m_{\text{bg}} \quad (10)
\end{aligned}$$

all involved probabilities can be rewritten as

$$P_{\text{bg}}^{(1)}(N) = \frac{b^N}{N!} \exp(-b) \quad (11)$$

$$P_{\text{bg}}^{(2)}(N_1, N_2) = \frac{(b/2)^{N_1+N_2}}{N_1! N_2!} \exp(-b) \quad (12)$$

$$\begin{aligned}
P_{\text{mol}}^{(1)}(N) &= \frac{1}{N!} \left\{ \int_0^{x_t} dx (\lambda x + b)^N \right. \\
&\quad \cdot \exp[-(1 + \lambda)x - b] \\
&\quad + (\lambda x_t + b)^N \\
&\quad \left. \cdot \exp[-(1 + \lambda)x_t - b] \right\} \quad (13)
\end{aligned}$$

and

$$\begin{aligned}
P_{\text{mol}}^{(2)}(N_1, N_2) &= \delta(N_2) \int_0^{x_t} dx \frac{1}{2N_1!} \left(\frac{\lambda x + b}{2} \right)^{N_1} \\
&\quad \cdot \exp \left[-\frac{(1 + \lambda)x - b}{2} \right] \\
&\quad + \frac{1}{N_1!} \left(\frac{\lambda x_t + b}{2} \right)^{N_1} \\
&\quad \cdot \exp \left[-\frac{(1 + \lambda)x_t - b}{2} \right] \\
&\quad \cdot \int_0^{x_t} dx \frac{1}{2N_2!} \left(\frac{\lambda x + b}{2} \right)^{N_2} \\
&\quad \cdot \exp \left[-\frac{(1 + \lambda)x - b}{2} \right] \\
&\quad + \frac{1}{N_1! N_2!} \left(\frac{\lambda x_t + b}{2} \right)^{N_1+N_2} \\
&\quad \cdot \exp[-(1 + \lambda)x_t - b]. \quad (14)
\end{aligned}$$

The computation of the corresponding MLF probability distributions can be done only numerically. Having these distributions in hand, one can easily compute the errors of detecting a molecule when no molecule is present (false positive) and of not detecting a molecule when it is present (false negative). This is done by setting a threshold value L_{th} of the MLF, and assuming there is a molecule to be detected if the corresponding MLF value is larger than this threshold, and assuming that no molecule is present when the MLF value is lower than this threshold. Thus, the error rates (for this given threshold value L_{th}) are

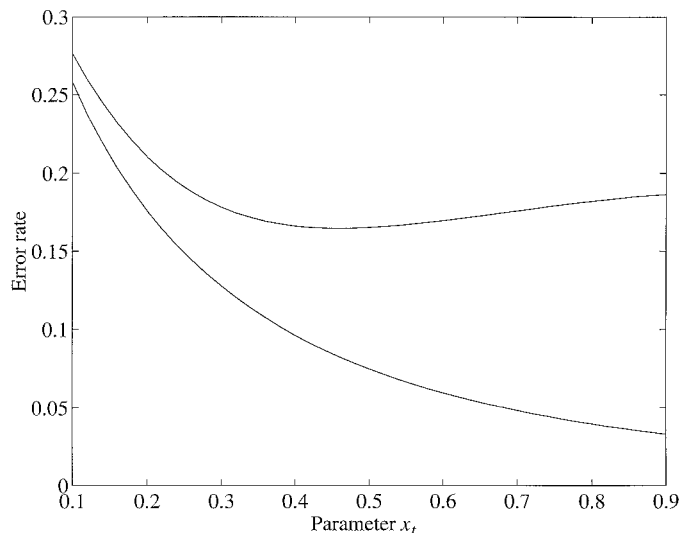


FIG. 2. Error rate for the one-focus (top) and two-foci (bottom) experiment. The parameters used were: $\lambda = 100$ and $b = 5\lambda x_r$.

$$\text{error} = \int_{L_{\text{th}}}^{\infty} dL P_{\text{bg}}^{(1,2)}(L) \quad (15)$$

for false positives and

$$\text{error} = \int_{-\infty}^{L_{\text{th}}} dL P_{\text{mol}}^{(1,2)}(L) \quad (16)$$

for false negatives. In the following calculations, the threshold value L_{th} was chosen in such a way that the errors for false positives and false negatives are equal. In Eqs. 11–14, there are three adjustable parameters: x_r , determining the bleaching rate, e^{-x_r} ; λ , determining, together with x_r , the mean number of detected photons; and b , giving the mean number of detected background photons. For our model calculations we fixed λ to be equal 100, and b was chosen in such a way that the maximum (no photobleaching) signal-to-background ratio, $(\lambda x_r + b)/b$, was always equal to 1.2. The only parameter varied was x_r . The result of the error calculations is shown in Fig. 2, for x_r varying between 0.1 and 0.9. As can be seen, photobleaching causes a difference in the detection errors for the one-focus and two-foci case (in contrast to the result of Eqs. 5 and 6). It appears at first glance that the two-foci setup has better detection efficiency than the one-focus setup. This is misleading. The reason for the improved error rate is that the two-foci setup provides more information about a single molecule's photobleaching dynamics by splitting the detection time into two parts. However, the same can be done in the one-focus case, simply by dividing the detection time t into two parts and counting the number of the detected photons separately for the time intervals $\{0, t/2\}$ and $\{t/2, t\}$. If the excitation profile is symmetric with respect to time $t/2$, then the corresponding photon detection probabilities are the same as in the two-foci setup, and also the error rates. Thus, the calculation shows that it is advantageous to look at the photon detection process with some time resolution

for decreasing the SMD error, but there is no advantage of using two foci as opposed to one.

In cases where molecular diffusion plays a role, the situation becomes even worse for the two-foci experiment, since when traveling from the first focus to the second there will always be a nonvanishing probability that the molecule diffuses away from the flow axis and misses the second focus. We also neglected dark counts in the detectors, since they can only worsen the situation for the two-foci setup.

In our above considerations we did not include optical saturation of the fluorescing molecule. Indeed, because of the convex shape of the saturation function one can expect to gather more fluorescence photons when exciting longer with a lower intensity. Thus, in a two-foci experiment one will receive more fluorescence photons than in a one-focus experiment with the same total laser intensity. But this result can be achieved, too, in the one-focus experiment by lowering the laser intensity and proportionally increasing the mean transit time (by decreasing the flow velocity) or by elongating the excitation region. Thus, again, the two-foci setup does not bring any improvement for the SMD efficiency.

ACKNOWLEDGMENTS

We thank W. Patrick Ambrose (LANL) for kindly reading the manuscript. J.E. gratefully acknowledges the support of the German Academic Exchange Service for granting him his stay with the Los Alamos National Laboratory and LANL for hosting his stay.

1. R. A. Keller, W. P. Ambrose, P. M. Goodwin, J. H. Jett, J. C. Martin, and M. Wu, *Appl. Spectrosc.* **50**, 12A (1996).
2. J. H. Jett, R. A. Keller, J. C. Martin, B. L. Marrone, R. K. Moyzis, R. L. Ratliff, N. K. Seitzinger, E. B. Shera, and C. C. Stewart, *J. Biomolec. Struct. and Dyn.* **7**, 301 (1989).
3. J. D. Harding, and R. A. Keller, *Trends in Biotech.* **10**, 55 (1992).
4. W. P. Ambrose, P. M. Goodwin, J. H. Jett, M. E. Johnson, J. C. Martin, B. L. Marrone, J. A. Schecker, C. W. Wilkerson, R. A. Keller, A. Haces, P.-J. Shih, and J. D. Harding, *Ber. Bunsenges. Phys. Chem.* **97**, 1535 (1993).
5. P. M. Goodwin, R. L. Affleck, W. P. Ambrose, J. N. Demas, J. H. Jett, J. C. Martin, L. J. Reha-Krantz, D. J. Semin, J. A. Schecker, M. Wu, and R. A. Keller, *Exp. Tech. Phys.* **41**, 279 (1995).
6. A. Castro, F. R. Fairfield, and E. B. Shera, *Anal. Chem.* **65**, 849 (1993).
7. P. M. Goodwin, M. E. Johnson, J. C. Martin, W. P. Ambrose, B. L. Marrone, J. H. Jett, and R. A. Keller, *Nucleic Acids Res.* **21**, 803 (1993).
8. J. T. Petty, M. E. Johnson, P. M. Goodwin, J. C. Martin, J. H. Jett, and R. A. Keller, *Anal. Chem.* **67**, 1755 (1995).
9. A. Castro and E. B. Shera, *Anal. Chem.* **67**, 3181 (1995).
10. A. Castro and E. B. Shera, *Appl. Opt.* **34**, 3218 (1995).
11. M. Eigen and R. Rigler, *Proc. Natl. Acad. Sci. USA* **91**, 5740 (1994).
12. R. Rigler, *J. Biotechnol.* **41**, 177 (1995).
13. D. Y. Chen, K. Adelhelm, X. L. Cheng, and N. J. Dovichi, *Analyst* **119**, 349 (1994).
14. D. Y. Chen and N. J. Dovichi, *Anal. Chem.* **68**, 690 (1996).
15. F. Zarrin and N. J. Dovichi, *Anal. Chem.* **57**, 2690 (1985).
16. L.-Q. Li and L. M. Davis, *Appl. Opt.* **34**, 3208 (1995).
17. E. B. Shera, N. K. Seitzinger, L. M. Davis, R. A. Keller, and S. A. Soper, *Chem. Phys. Lett.* **174**, 553 (1990).
18. R. D. Guenard, Y. H. Lee, M. Bolshov, D. Hueber, B. W. Smith, and J. D. Winefordner, *Appl. Spectrosc.* **50**, 188 (1996).
19. M. Köllner, *Appl. Opt.* **32**, 806 (1993).
20. J. Enderlein, *Proc. SPIE* **2136**, 226 (1994).
21. J. Enderlein, *Appl. Opt.* **34**, 514 (1995).